

Dalton Transactions

Accepted Manuscript



This is an *Accepted Manuscript*, which has been through the Royal Society of Chemistry peer review process and has been accepted for publication.

Accepted Manuscripts are published online shortly after acceptance, before technical editing, formatting and proof reading. Using this free service, authors can make their results available to the community, in citable form, before we publish the edited article. We will replace this *Accepted Manuscript* with the edited and formatted *Advance Article* as soon as it is available.

You can find more information about *Accepted Manuscripts* in the [Information for Authors](#).

Please note that technical editing may introduce minor changes to the text and/or graphics, which may alter content. The journal's standard [Terms & Conditions](#) and the [Ethical guidelines](#) still apply. In no event shall the Royal Society of Chemistry be held responsible for any errors or omissions in this *Accepted Manuscript* or any consequences arising from the use of any information it contains.



ARTICLE

Large-Scale Delamination of Multi-Layers Transition Metal Carbides and Carbonitrides “MXenes”

Michael Naguib,^{*a} Raymond R. Unocic,^b Beth L. Armstrong,^a and Jagjit Nanda^a

Received 00th January 20xx,
Accepted 00th January 20xx

DOI: 10.1039/x0xx00000x

www.rsc.org/

Herein we report on a general approach to delaminate multi-layered MXenes using an organic base to induce swelling that in turn weakens the bonds between the MX layers. Simple agitation or mild sonication of the swollen MXene in water resulted in the large-scale delamination of the MXene layers. The delamination method is demonstrated for vanadium carbide and titanium carbonitride MXenes.

Introduction

Two-dimensional (2D) layers of transition metal carbides and carbonitrides, so-called “MXenes”, are synthesized by etching atomically thin metal layers from “MAX phases”.¹⁻⁴ The latter is a large family of hexagonal layered, $P6_3/mmc$, ternary transition metal (TM) carbides and/or nitrides with a composition of $M_{n+1}AX_n$ where M stands for a transition metal (Sc, Ti, V, Cr, Nb, Mo, etc.), A are group 13 and 14 elements (Al, Si, Sn, In, etc.), X is carbon or nitrogen, and $n = 1, 2, \text{ or } 3$.⁵ MXenes are both hydrophilic and good electrical conductors,² a rare combination in 2D materials. Despite their short materials development history, the exploratory use of MXenes in many applications shows great promise due to their inherent physiochemical properties. For example, excellent volumetric capacitances were reported for Ti_3C_2 when tested as electrodes for electrochemical supercapacitors.⁶⁻⁸ MXenes also exhibit good capacity and rate capability when used as electrodes for Li-ion batteries (LIBs) and Li-ion capacitors.^{3, 9-13} MXenes were found to be good supports for catalysts.¹⁴⁻¹⁶ Water purification is another venue where MXenes show great promise since they can selectively remove lead¹⁷ and chromium (VI)¹⁸ from water. MXenes could be used also as a precursor for novel hybrid structures of nanoscale transition metal oxides on carbon.¹⁹ Theoretical calculations also predict other possible applications for MXenes, e.g. some MXenes are predicted to have good thermoelectric properties,^{20, 21} and also in principle could be used as anodes for other ion batteries including Ca, K, Na,^{22, 23} Mg and Al.²³

During MXenes synthesis, the aluminum, Al, in the MAX phase is replaced by a mixture of functional groups (OH, O, and F; represented hereafter by T_x). The latter weakens the bonding between $M_{n+1}X_n$ layers which then allows sonication to separate the layers from each other.²⁴ However, the low yields of delaminated

flakes are too small to be used in many applications where fully delaminated layers are required, such as in polymer reinforcements. Thus, most of the explored applications for MXenes have focused on stacked MXenes multi-layered powders,^{3, 9, 10, 14, 22} i.e. not fully delaminated ones. To date the only exception has been $Ti_3C_2T_x$, that was delaminated by the intercalation of dimethylsulfoxide (DMSO) followed by sonication in water.²⁵ This procedure resulted in delaminated $Ti_3C_2T_x$ layers, which form a stable colloidal solution in water. For reasons that are not obvious, this approach has only been successful with $Ti_3C_2T_x$ since DMSO does not appear to intercalate other MXenes. Another approach to delaminate $Ti_3C_2T_x$ was achieved by treating Ti_3AlC_2 with a mixture of hydrochloric acid, HCl, and lithium fluoride, LiF, instead of using HF directly.⁷ Sonication materials synthesized by this approach in water resulted in a colloidal solution of delaminated $Ti_3C_2T_x$ in water. Again, this approach to date has only been successful with $Ti_3C_2T_x$. The successful delamination of $Ti_3C_2T_x$ allowed them to be used in composites^{26, 27} that showed excellent performance as electrodes for LIBs and electrochemical capacitors. Also, flexible additive-free delaminated $Ti_3C_2T_x$ ‘paper’ with an outstanding volumetric capacitance, was produced by simply filtering the colloidal solutions.^{6, 8} Ammonium bifluoride, NH_4HF_2 , was used successfully to etch Al from Ti_3AlC_2 instead of HF, but this technique did not result in delaminating the resulted MXene.²⁸

Unlike mechanical delamination techniques, such as using Scotch tape,^{29, 30} liquid delamination of layered materials is an effective and simple technique for large-scale production of 2D materials that can be used in many applications that vary from reinforcements in polymers to energy storage and catalysis.³¹ Many 2D materials were successfully produced by liquid delamination, such as graphene,^{32, 33} transition metal dichalcogenides (TMDs), boron nitride,³⁴ TM oxides and hydroxides.³⁵ For most of these examples, the weak out-of-plane van der Waals bonds between the layers in the parent 3D materials can be easily broken by sonication in certain solvents resulting in stable colloidal solution of 2D layers. In the case of layered TM oxides and hydroxides, extra steps of exchanging alkali metal cations in-between the layers with protons, followed by replacing the protons with large organic cations, such as tetrabutylammonium (TBA) are needed. The latter step is

^a Materials Science and Technology Division, Oak Ridge National Laboratory, Oak Ridge, TN 37831, USA. Fax: +1 865-576-6298; Tel: +1 865-574-5977; E-mail: naguibma@ornl.gov

^b Center for Nanophase Materials Science, Oak Ridge National Laboratory, Oak Ridge, TN 37831, USA. Address here.

[†] Electronic Supplementary Information (ESI) available: Experimental details for the synthesis of MAX phases and MXenes in addition to characterization techniques. See DOI: 10.1039/x0xx00000x

accompanied by a significant swelling of the layered TM oxides that in turn facilitates the delamination process. Recently, Jeong *et al.*³⁶ reported on a similar "Tandem" intercalation of Lewis base to effectively delaminate TMDs.

Herein we report a general approach for the large-scale delamination of MXenes using a relatively large organic base, namely tetrabutylammonium hydroxide (TBAOH), choline hydroxide, or *n*-butylamine. These bases react with the MXenes resulting in intercalated MXenes with a large increase in the *d*-spacing, *i.e.* swollen MXene, compared to pristine as-synthesized MXenes (Fig. 1). Hand shaking the intercalated MXenes in water resulted in stable colloidal solutions of delaminated flakes. As shown in Fig. 1 the process is highly scalable (from mL to L) to produce large quantities of colloidal solutions. Unlike the previously reported procedures for the delamination of $\text{Ti}_3\text{C}_2\text{T}_x$, the approach described here is much more universal, since it successfully delaminated many MXenes, not just a single composition, using several organic bases. Also, as a result of the organic base treatment of MXenes during the delamination process, the F-content in the MXenes was significantly reduced/eliminated which is an important step toward controlling the surface chemistry of MXenes. Although the volumes produced here are not at the industrial scale, the simplicity of the delamination process shows a potential for a straight forward scale-up.

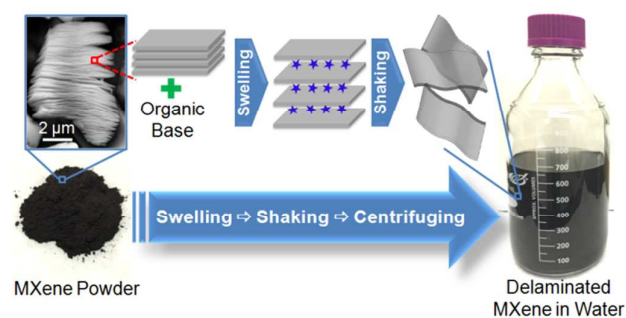


Fig. 1 Schematic for MXene delamination process by reacting MXenes with an organic base that causes multilayered MXene powder (pictured in bottom left) to swell significantly. Then by simply hand shaking or mild sonication in water the layers delaminate forming a stable colloidal solution (right side). A typical SEM image of the as synthesized Ti_3CNT_x multi-layer MXene is shown top left.

V_2CT_x and Ti_3CNT_x were used as examples for MXenes that could be delaminated using this technique. The rationale behind selecting V_2CT_x for this study as a representative M_2X MXene, was the fact that it showed the highest Li uptake when tested as electrodes for LIBs compared to all the other multi-layer MXenes.³ Thus, delaminated V_2CT_x could be useful for application in LIB batteries. Ti_3CNT_x was selected in this study, since it behaves differently from $\text{Ti}_3\text{C}_2\text{T}_x$ but has the same transition metal and the same number of atomic layers (per single MXene sheet). For example, the change in *c*-lattice parameter, Δc -LP, upon the conversion from MAX phase to MXene is about 50% higher in the case of Ti_3CNT_x (~ 3 Å) compared to $\text{Ti}_3\text{C}_2\text{T}_x$ (~ 2 Å). Also, the $\text{Ti}_3\text{C}_2\text{T}_x$ could be intercalated with DMSO and delaminated while Ti_3CNT_x could not be.

Experimental

A detailed description for the synthesis of the MAX phases (V_2AlC and Ti_3AlCN), their corresponding MXenes (V_2CT_x and Ti_3CNT_x), and the organic base treatment of MXenes as well as the details for the characterization techniques used in this work are given in the electronic supplementary information (ESI†). Briefly, MXene powders were mixed with an aqueous solution of 54-56% TBAOH, $(\text{C}_4\text{H}_9)_4\text{NOH}$, (Sigma Aldrich, St. Louis, MO, USA) in a ratio of 1g MXene to 10mL base solution. The mixture was then stirred at room temperature (RT) for 2, 4 or 21 h.

After the prescribed mixing time, the mixtures were centrifuged at 2000 rpm for 0.5 h. The supernatant liquids were then decanted, and the sediment was used for further characterization and delamination. More details about the delamination process can be found in the ESI†. In short, mixtures of DI water with MXenes (1 g of MXene : 400 mL of DI) were either hand-shaken for 2 minutes (for V_2CT_x) or sonicated for 20 minutes (for Ti_3CNT_x). Then, the solutions were centrifuged at 2000 rpm for 0.5 h, and the black supernatants were decanted and used for further investigation.

Results and Discussion

In order to ascertain the surface charge and the fundamental interaction of the delaminated MXene layers with water, zeta potential measurements were performed as a function of pH.

As shown in Fig. 2, zeta potential (ζ) measurement for Ti_3CNT_x at different pH values showed a negatively charged particle behavior at neutral and basic pH, which is similar to what was reported for $\text{Ti}_3\text{C}_2\text{T}_x$.¹⁸ At a pH of 11.7, a ζ of -77 mV was recorded, while in the pH range of 6.2 to 8.3, ζ varied from -51 to -71 mV. The midrange of those ζ values is almost twice as negative compared to what was reported for $\text{Ti}_3\text{C}_2\text{T}_x$ at a pH of 7 (~ -29 mV)¹⁸ which explains why Ti_3CNT_x appears to form a more stable colloidal solution in water as compared to $\text{Ti}_3\text{C}_2\text{T}_x$. The point of zero charge (PZC) of Ti_3CNT_x was found to be 3.3 which is higher than that of $\text{Ti}_3\text{C}_2\text{T}_x$ (2.4).¹⁸ For V_2CT_x , the particles were found to be negatively charged within the entire range of pH we tested at (from 0.97 to 11.3), and the zeta potential curve did not cross the PZC line. Around neutral pH, in the range of 6.06 to 8.00, the ζ were found to be in the range of -46 mV to -58 mV.

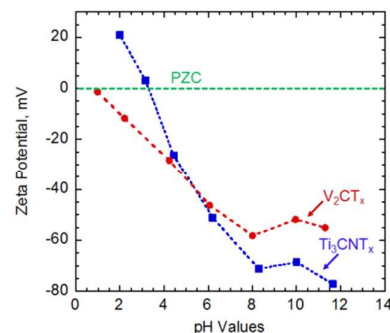


Fig. 2 Zeta potential dependence on pH for Ti_3CNT_x (blue curve with square points) and V_2CT_x (red curve with round points) multi-layer powders with a concentration of 1 mg/mL. The horizontal green dashed line indicates the position of zero zeta potential, which intersects with the zeta potential plot at the point of zero charge (PZC).

The XRD patterns for Ti_3CNT_x before and after TBAOH treatment, after various mixing times, are shown in Fig. 3A. A significant shift in the 0002 peak of Ti_3CNT_x from 2θ of 8.26° to 4.57° after 2 h of treatment in the TBAOH solution was observed. This shift corresponds to an increase of the *c*-LP from 21.4 Å to 38.6 Å. After 4 h of mixing, the 0002 peak shifted to a 2θ of 4.5° that corresponds to *c*-LP of 39.2 Å ($\Delta c\text{-LP} \sim 17.9\text{Å}$, $\Delta d\text{-spacing} \sim 8.9\text{Å}$). Mixing for 21 h did not result in further increase in the *c*-LPs. It follows that 4 h is a sufficient time to achieve maximum spontaneous swelling in the Ti_3CNT_x case in a 54-56% TBAOH aqueous solution at RT. Spontaneous intercalation of alkali metal hydroxide in aqueous system was reported for $\text{Ti}_3\text{C}_2\text{T}_x$, and the maximum reported increase in the *c*-LP in the case of KOH was about 5.1 Å.⁸ Not surprisingly, given the large size differences between K^+ and TBA^+ , the increase reported here is significantly larger.

For V_2CT_x (Fig. 3B), the 0002 peak shifted from a 2θ of 8.9° to 4.6° (*c*-LP from 19.9 Å to 38.6 Å) after 2 h mixing in TBAOH solution. By doubling the time to 4 h, a very slight down shift in the 0002 peak position was observed (shifted down to 4.56°). This new peak location corresponds to a *c*-LP of 38.72 Å. The overall increase in the *d*-spacing was $\sim 9.4\text{Å}$. It is worth noting that the 0004 and 0006 peaks appeared after the TBAOH treatments. Also, a smaller broad shoulder for the 0002 peak at 2θ around 5.6° appeared after the TBAOH treatment. As shown in Fig. S1 (ESI†), other strong organic bases, such as choline hydroxide, $(\text{C}_5\text{H}_{14}\text{NO})\text{OH}$, and even weak bases like *n*-butylamine, $\text{C}_4\text{H}_{11}\text{N}$, were found to induce swelling in V_2CT_x but less than what was observed for TBAOH (the *c*-LP after 4 h treatment was found to be 36.0 Å for 50% aqueous choline hydroxide V_2CT_x and 36.3 Å for *n*-butylamine treated V_2CT_x). More details about the other bases treatments are given in the ESI†.

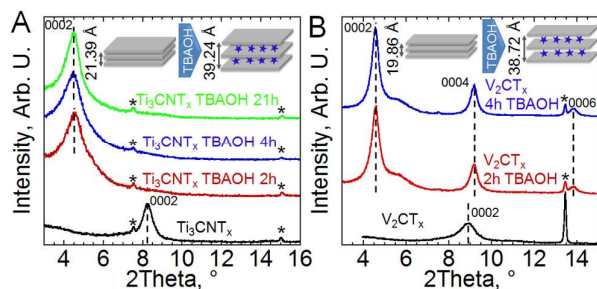


Fig. 3 XRD patterns for: (A) Ti_3CNT_x before (black pattern at bottom) and after mixing with TBAOH for 2, 4, and 21 h (red, blue, and green, respectively). (B) V_2CT_x before (black pattern at bottom) and after mixing with TBAOH for 2 and 4 h (red and blue patterns respectively). The peaks denoted by * are those for the un-reacted MAX phase; in A that phase is $\text{Ti}_4\text{Al}(\text{C,N})_3$, in B it is V_2AlC . The insets are schematics of the MXene unit cells before, and after, TBAOH intercalation with the corresponding change in the *c* lattice parameter.

By adding water to the TBAOH treated V_2CT_x samples followed by hand shaking, a black colloidal solution was formed. The solution was still black even after centrifuging (Fig. 4A). By shining a laser beam into the solution (inset Fig. 4B), we noticed the Tyndall effect thereby confirming it to be a colloidal solution. It is worth noting that both samples treated using choline hydroxide and *n*-butylamine formed very similar black colloidal solutions using the procedure described above for TBAOH treated samples. This indicates that other organic bases (either strong or weak) can also be used to delaminate MXenes.

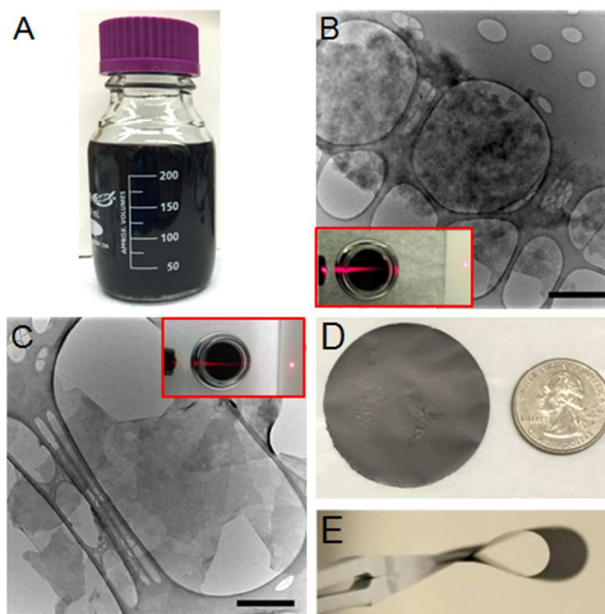


Fig. 4 (A) Photograph of a glass bottle filled with delaminated V_2CT_x in water after centrifuging. (B) TEM image of a delaminated V_2CT_x flake. Inset shows the Tyndall effect for this mixture. (C) TEM image of a delaminated Ti_3CNT_x flakes (the inset is a photograph for vial of delaminated Ti_3CNT_x colloidal solution, after centrifuging, showing a Tyndall effect). Scale bars in B and C are equal to 1 μm (D) Photograph of additives free Ti_3CNT_x paper fabricated by vacuum-filtering the colloidal solution of delaminated Ti_3CNT_x (US quarter dollar coin added for size comparison). (E) A photograph of the same paper shown in D, but bent and held using tweezers.

Fig. 4B shows a TEM image for a delaminated V_2CT_x flake after the TBAOH treatment. The electron energy loss spectroscopy (EELS) analysis of this flake (Fig. S2A, ESI†) indicated the presence of V, C, and O. A high density of holes within the V_2CT_x flakes was observed in most of the investigated samples. Those holes were either formed during the TBAOH treatment or after delamination in water. The latter is more likely since the XRD peaks of the TBAOH treated powders were relatively narrow and more intense which does not agree with a more defective structure. Also, it was noticed that the color of V_2CT_x colloidal solution turned from black to yellow, as shown in Fig. S3 (ESI†), by just storing the solution in air for 48 h. The yellow color is characteristic for solutions contacting pentavalent V (i.e. VO_2^+ , or VO_3^-). This change in color was accompanied with a reduction of the pH from neutral to values ~ 4 . No Tyndall effect was observed for the yellow solution, which can be taken as evidence for the disappearance of the V_2CT_x flakes. In other words, the delaminated V_2CT_x was completely dissolved in water. Although vanadium carbide is known to be stable in water, vanadium oxide is not. Thus, it is reasonable to assume that the dissolution is taking place in two steps: oxidation followed by dissolution. Similar oxidation of delaminated $\text{Ti}_3\text{C}_2\text{T}_x$ in water was observed, but since titanium oxide is stable in water, white sediment was obtained.¹⁸ Consistent with this conjecture is the fact that when the vial was completely filled with the black, delaminated V_2CT_x solution and the lid was sealed, no change in color was observed over the same time period. This indicates that, like in the case of $\text{Ti}_3\text{C}_2\text{T}_x$, dissolved oxygen in the water must play an important role in the dissolution of delaminated V_2CT_x . To avoid this problem, either the water needs to be replaced with other solvents

or the V_2CT_x colloidal solutions need to be used right away after preparation. In the absence of water, the flakes are much more resistant to oxidation.

Sonicated the Ti_3CNT_x that was pretreated with TBAOH for 4h, in water for 20 minutes, followed by centrifuging, to separate delaminated Ti_3CNT_x colloidal solution from the non-delaminated settled MXene, resulted in a black colloidal solution (see photograph on right in Fig. 1). A similar colloidal solution was obtained for the powders mixed with TBAOH for 21 h. Here again, hand-shaking was sufficient to form a stable colloidal solution even after centrifuging but we decided to use sonication to ensure reproducibility. As shown in the inset of Fig. 4C the diluted colloidal solution showed a clear Tyndall effect. Investigating this delaminated Ti_3CNT_x using TEM, showed a significant amount of MXene flakes. Fig. 4C shows one of those flakes with many smaller flakes laying on top of it. The EELS spectrum of this flake (Fig. S2B, ESI†) showed peaks for Ti, C, N, and O.

Filtering the colloidal solution of delaminated Ti_3CNT_x resulted in a free-standing additive-free flexible paper (Fig. 4D-E). Similar paper was reported for $Ti_3C_2T_x$ and found to have outstanding performances in LIBs²⁵ and supercapacitors.⁸ When the same filtering procedure was repeated but using delaminated V_2CT_x solution, the resulting paper disintegrated and crumbled upon drying in air. Other MXene 'paper', such as $Ta_4C_3T_x$, was successfully fabricated using the same delamination procedure described herein, but due to space limitations these results will be presented in a standalone paper.

Comparing the energy-dispersive X-ray spectroscopy analysis (Table S1, ESI†) for samples before and after delamination shows a significant reduction in the F content, while the oxygen content was found to increase after delamination. In case of Ti_3CNT_x the atomic ratio of Ti:O:F changed from ~ 3.0:1.5:2.0 for as the synthesized MXene powder (before any treatment) to ~ 3.0:3.6:0.8 after delamination. For V_2CT_x , the F was almost eliminated completely after delamination and V:O:F atomic ratio changed from 2.0:1.1:1.0 for as synthesized V_2CT_x powder to 2.0:3.1:0.0 for delaminated MXene. Although EDS results showed, qualitatively, that F content was reduced while O content was increased after delamination, more work is needed to accurately quantify the F and O contents in MXenes. Similar reduction in the F content was observed for $Ti_3C_2T_x$ when treated with KOH⁶ and it was explained by a replacement reaction between KOH and F termination. The same analogy could be used to explain the reduction of the F content upon TBAOH treatment followed by delamination. Theoretical calculations predict that F termination is less stable compared to O and OH.³⁷ Thus in presence of base compound, the F termination, in principle, could be easily replaced by OH, forming a water soluble fluoride compound. Replacing F by O or OH is very useful for controlling the surface chemistry of MXenes, which had been a challenge since their rise in 2011. The ability to reduce/eliminate the F content in the delaminated MXene is another advantage of the delamination approach described here.

Conclusions

In summary, treating multi-layer MXenes powders with the organic base, TBAOH, at room temperature resulted in significant and spontaneous swelling that in turn weakens the van der Waals' bonds between MXene layers. Once the TBAOH intercalates the MXene flakes, slight agitation or mild sonication results in their

delamination. The MXenes are highly negatively charged and form stable colloidal solutions in water as confirmed by zeta potential measurements. Unlike the previously reported approach to delaminate $Ti_3C_2T_x$ using DMSO, this approach is more universal for different MXenes and different organic bases and can potentially yield large quantities of delaminated MXenes. In this study, V_2CT_x and Ti_3CNT_x were used as examples for MXenes (with different composition and number of atomic layers) that could be delaminated using the organic base treatment. Similar to TBAOH, other organic bases including choline hydroxide and n-butylamine resulted in successful delamination of V_2CT_x . Delaminated V_2CT_x was found to have a high susceptibility for oxidation in water in the presence of air, thereby forming the water-soluble pentavalent oxide. Free-standing additive-free flexible paper of Ti_3CNT_x was produced by filtering the colloidal solution of delaminated MXene. Using this approach, the delaminated MXenes showed a significant reduction in the F-content. Delaminating MXenes with various compositions in large-scales and replacing the F-content by oxygen will open the door for many applications that have not been explored for MXenes yet.

Acknowledgements

This work was supported by the Laboratory Directed Research and Development Program of Oak Ridge National Laboratory, managed by UT-Battelle, LLC, for the U.S. Department of Energy. Microscopy conducted as part of a user proposal at ORNL's Center for Nanophase Materials Sciences (CNMS), which is an Office of Science User Facility

Notes and references

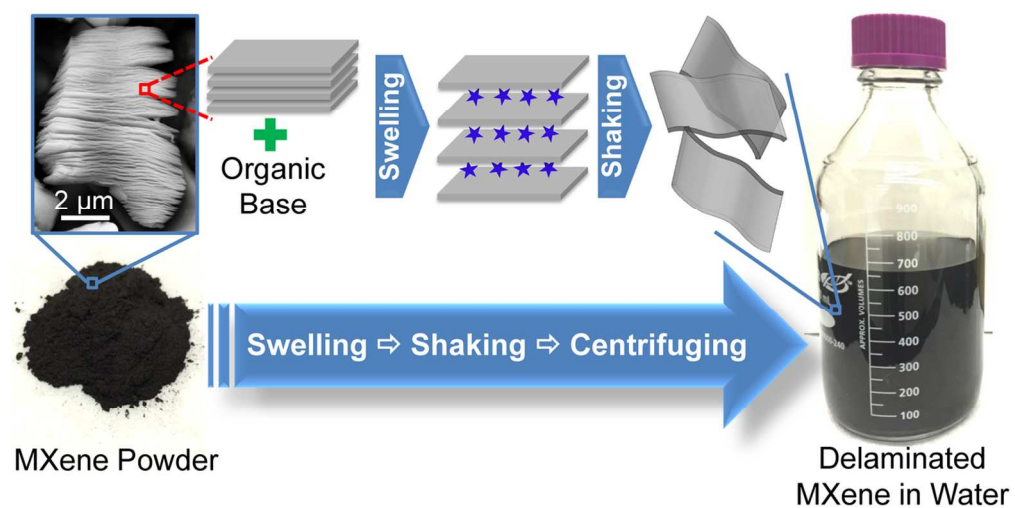
^a Materials Science and Technology Division, Oak Ridge National Laboratory, Oak Ridge, TN 37831, USA. Fax: +1 865-576-6298; Tel: +1 865-574-5977; E-mail: naguibma@ornl.gov

^b Center for Nanophase Materials Science, Oak Ridge National Laboratory, Oak Ridge, TN 37831, USA.

† Electronic Supplementary Information (ESI) available: Experimental details for the synthesis of MAX phases and MXenes in addition to characterization techniques. See DOI: 10.1039/b000000x/

- 1 M. Naguib, M. Kurtoglu, V. Presser, J. Lu, J. Niu, M. Heon, L. Hultman, Y. Gogotsi and M. W. Barsoum, *Adv. Mater.*, 2011, **23**, 4248-4253.
- 2 M. Naguib, O. Mashtalir, J. Carle, V. Presser, J. Lu, L. Hultman, Y. Gogotsi and M. W. Barsoum, *ACS Nano*, 2012, **6**, 1322-1331.
- 3 M. Naguib, J. Halim, J. Lu, K. M. Cook, L. Hultman, Y. Gogotsi and M. W. Barsoum, *J. Am. Chem. Soc.*, 2013, **135**, 15966-15969.
- 4 M. Ghidui, M. Naguib, C. Shi, O. Mashtalir, L. M. Pan, B. Zhang, J. Yang, Y. Gogotsi, S. J. L. Billinge and M. W. Barsoum, *Chem. Commun.*, 2014, **50**, 9517-9520.
- 5 M. W. Barsoum, *MAX Phases: Properties of Machinable Ternary Carbides and Nitrides*, John Wiley & Sons, Weinheim, Germany, 2013.
- 6 Y. Dall'Agnese, M. R. Lukatskaya, K. M. Cook, P.-L. Taberna, Y. Gogotsi and P. Simon, *Electrochem. Commun.*, 2014, **48**, 118-122.
- 7 M. Ghidui, M. R. Lukatskaya, M.-Q. Zhao, Y. Gogotsi and M. W. Barsoum, *Nature*, 2014, **516**, 78-81.
- 8 M. R. Lukatskaya, O. Mashtalir, C. E. Ren, Y. Dall'Agnese, P. Rozier, P. L. Taberna, M. Naguib, P. Simon, M. W. Barsoum and Y. Gogotsi, *Science*, 2013, **341**, 1502-1505.

- 9 J. Come, M. Naguib, P. Rozier, M. W. Barsoum, Y. Gogotsi, P.-L. Taberna, M. Morcrette and P. Simon, *J. Electrochem. Soc.*, 2012, **159**, A1368-A1373.
- 10 M. Naguib, J. Come, B. Dyatkin, V. Presser, P.-L. Taberna, P. Simon, M. W. Barsoum and Y. Gogotsi, *Electrochem. Commun.*, 2012, **16**, 61-64.
- 11 D. Sun, M. Wang, Z. Li, G. Fan, L.-Z. Fan and A. Zhou, *Electrochem. Commun.*, 2014, **47**, 80-83.
- 12 Q. Tang and Z. Zhou, *Prog. Mater. Sci.*, 2013, **58**, 1244-1315.
- 13 Q. Tang, Z. Zhou and P. Shen, *J. Am. Chem. Soc.*, 2012, **134**, 16909-16916.
- 14 Y. Gao, L. Wang, Z. Li, A. Zhou, Q. Hu and X. Cao, *Solid State Sci.*, 2014, **35**, 62-65.
- 15 X. Xie, S. Chen, W. Ding, Y. Nie and Z. Wei, *Chem. Commun.*, 2013, **49**, 10112-10114.
- 16 X. Li, G. Fan and C. Zeng, *Int. J. Hydrogen Energy*, 2014, **39**, 14927-14934.
- 17 Q. Peng, J. Guo, Q. Zhang, J. Xiang, B. Liu, A. Zhou, R. Liu and Y. Tian, *J. Am. Chem. Soc.*, 2014, **136**, 4113-4116.
- 18 Y. Ying, Y. Liu, X. Wang, Y. Mao, W. Cao, P. Hu and X. Peng, *ACS Appl. Mater. Interfaces*, 2015, **7**, 1795-1803.
- 19 M. Naguib, O. Mashtalir, M. R. Lukatskaya, B. Dyatkin, C. Zhang, V. Presser, Y. Gogotsi and M. W. Barsoum, *Chem. Commun.*, 2014, **50**, 7420-7423.
- 20 M. Khazaei, M. Arai, T. Sasaki, C.-Y. Chung, N. S. Venkataramanan, M. Estili, Y. Sakka and Y. Kawazoe, *Adv. Funct. Mater.*, 2013, **23**, 2185-2192.
- 21 M. Khazaei, M. Arai, T. Sasaki, M. Estili and Y. Sakka, *Phys. Chem. Chem. Phys.*, 2014, **16**, 7841-7849.
- 22 Y. Xie, Y. Dall'Agnese, M. Naguib, Y. Gogotsi, M. W. Barsoum, H. L. Zhuang and P. R. C. Kent, *ACS Nano*, 2014, **8**, 9606-9615.
- 23 D. Er, J. Li, M. Naguib, Y. Gogotsi and V. B. Shenoy, *ACS Appl. Mater. Interfaces*, 2014, **6**, 11173-11179.
- 24 M. Naguib, V. N. Mochalin, M. W. Barsoum and Y. Gogotsi, *Adv. Mater.*, 2014, **26**, 992-1005.
- 25 O. Mashtalir, M. Naguib, V. N. Mochalin, Y. Dall'Agnese, M. Heon, M. W. Barsoum and Y. Gogotsi, *Nat. Commun.*, 2013, **4**, 1716.
- 26 Z. Ling, C. E. Ren, M. Zhao, J. Yang, J. M. Giammarco, J. Qiu, M. W. Barsoum and Y. Gogotsi, *Proc. Natl. Acad. Sci. U.S.A.*, 2014, **111**, 16676-16681.
- 27 M.-Q. Zhao, C. E. Ren, Z. Ling, M. R. Lukatskaya, C. Zhang, K. L. Van Aken, M. W. Barsoum and Y. Gogotsi, *Adv. Mater.*, 2015, **27**, 339-345.
- 28 J. Halim, M. R. Lukatskaya, K. M. Cook, J. Lu, C. R. Smith, L.-Å. Näslund, S. J. May, L. Hultman, Y. Gogotsi, P. Eklund and M. W. Barsoum, *Chem. Mater.*, 2014, **26**, 2374-2381.
- 29 K. S. Novoselov, A. K. Geim, S. V. Morozov, D. Jiang, Y. Zhang, S. V. Dubonos, I. V. Grigorieva and A. A. Firsov, *Science*, 2004, **306**, 666-669.
- 30 K. S. Novoselov, D. Jiang, F. Schedin, T. J. Booth, V. V. Khotkevich, S. V. Morozov and A. K. Geim, *Proc. Natl. Acad. Sci. U.S.A.*, 2005, **102**, 10451-10453.
- 31 V. Nicolosi, M. Chhowalla, M. G. Kanatzidis, M. S. Strano and J. N. Coleman, *Science*, 2013, **340**, 1226419.
- 32 X. Wang, P. F. Fulvio, G. A. Baker, G. M. Veith, R. R. Unocic, S. M. Mahurin, M. Chi and S. Dai, *Chem. Commun.*, 2010, **46**, 4487-4489.
- 33 Y. Hernandez, V. Nicolosi, M. Lotya, F. M. Blighe, Z. Sun, S. De, I. McGovern, B. Holland, M. Byrne and Y. K. Gun'ko, *Nat. Nanotechnol.*, 2008, **3**, 563-568.
- 34 J. N. Coleman, M. Lotya, A. O'Neill, S. D. Bergin, P. J. King, U. Khan, K. Young, A. Gaucher, S. De, R. J. Smith, I. V. Shvets, S. K. Arora, G. Stanton, H.-Y. Kim, K. Lee, G. T. Kim, G. S. Duesberg, T. Hallam, J. J. Boland, J. J. Wang, J. F. Donegan, J. C. Grunlan, G. Moriarty, A. Shmeliov, R. J. Nicholls, J. M. Perkins, E. M. Grieveson, K. Theuvsissen, D. W. McComb, P. D. Nellist and V. Nicolosi, *Science*, 2011, **331**, 568-571.
- 35 R. Ma and T. Sasaki, *Acc. Chem. Res.*, 2015, **48**, 136-143.
- 36 S. Jeong, D. Yoo, M. Ahn, P. Miró, T. Heine and J. Cheon, *Nat Commun*, 2015, **6**, 5763.
- 37 Y. Xie, M. Naguib, V. N. Mochalin, M. W. Barsoum, Y. Gogotsi, X. Yu, K.-W. Nam, X.-Q. Yang, A. I. Kolesnikov and P. R. C. Kent, *J. Am. Chem. Soc.*, 2014, **136**, 6385-6394.



Large-scale delamination of MXenes was achieved by using a simple aqueous organic base treatment followed by agitation in water.
117x58mm (300 x 300 DPI)